PRAMANA — journal of physics

Vol. 85, No. 2
August 2015
pp. 315–322

Non-compound nucleus fission in actinide and pre-actinide regions

R TRIPATHI*, S SODAYE and K SUDARSHAN
Radiochemistry Division, Bhabha Atomic Research Centre, Mumbai 400 085, India
*Corresponding author. E-mail: rahult@barc.gov.in

DOI: 10.1007/s12043-015-1045-1; ***e*Publication:** 22 July 2015

Abstract. In this article, some of our recent results on fission fragment/product angular distributions are discussed in the context of non-compound nucleus fission. Measurement of fission fragment angular distribution in ^{28}Si+^{176}Yb reaction did not show a large contribution from the non-compound nucleus fission. Data on the evaporation residue cross-sections, in addition to those on mass and angular distributions, are necessary for better understanding of the contribution from non-compound nucleus fission in the pre-actinide region. Measurement of mass-resolved angular distribution of fission products in ^{20}Ne+^{232}Th reaction showed an increase in angular anisotropy with decreasing asymmetry of mass division. This observation can be explained based on the contribution from pre-equilibrium fission. Results of these studies showed that the mass dependence of anisotropy may possibly be used to distinguish pre-equilibrium fission and quasifission.

Keywords. Fission; angular distribution; non-compound nucleus fission.

PACS Nos 25.70.Jj; 25.85.Ge

1. Introduction

Study of non-compound nucleus fission has been an important subject of recent studies in the area of heavy-ion fusion. Entrance-channel dynamics as well as potential energy landscape play important roles in governing the contribution from these processes. Saddle-point shapes and energies are very different in pre-actinide and actinide regions. In the pre-actinide region, saddle point is very elongated and higher in energy compared to that in the heavy actinide region. In this mass region, non-compound nucleus fission is expected to be observed with relatively heavier projectiles compared to that in heavy actinide region. At beam energies, not much above the entrance-channel Coulomb barrier, so that maximum angular momentum ($\ell_{\max}$) populated in the reaction is lower than ℓ_{Bf} (angular momentum for which fission barrier vanishes), non-compound nucleus fission process may be of two types, namely, pre-equilibrium fission [1,2] and quasifission [3]. In pre-equilibrium fission, fission occurs before complete equilibration in K-degree of

freedom (projection of total angular momentum on nuclear symmetry axis). In quasifission, the composite or dinuclear system formed after the collision of the projectile and the target nuclei escapes in the exit fission channel without being captured inside the unconditional saddle point [3]. Contribution from pre-equilibrium fission leads to a larger angular anisotropy compared to that predicted by the statistical saddle-point model (SSPM) [4,5]. For the reaction systems having contribution from non-compound nucleus fission, broadening or asymmetric component in the fission fragment mass distribution [6–12] as well as anomalous fission fragment angular distributions [1,2,13–16] are reported. In spite of extensive studies on non-compound nucleus fission in pre-actinide as well as actinide regions, there are several aspects which are not well understood. It is not clearly understood whether non-compound nucleus fission is always coupled to a suppression in the formation of evaporation residues compared to the prediction of statistical theory for compound nucleus (CN) decay. This ambiguity arises due to the lack of a complete theory unifying the entrance and exit channels which can simultaneously explain various types of fission processes and formation of evaporation residues. The second aspect is the distinction between pre-equilibrium and quasifission process as both these processes lead to an anomalous fission fragment angular distribution. Pre-equilibrium fission differs from quasifission in that, unlike in quasifission, fissioning system encounters a fission barrier on its way to fission, though the time-scale is not sufficient enough to achieve a fully equilibrated K-distribution as expected for compound nucleus fission. One would expect pre-equilibrium fission to lie between compound nucleus fission and quasifission in terms of equilibration in various degrees of freedom.

For a better understanding of these issues, it would be required to measure various observables such as fission fragment mass and angular distributions, and evaporation residue cross-section for each given reaction while covering a wide range of entrance channel mass asymmetry. It should be mentioned here that, for reaction systems with large entrance-channel Coulomb repulsion (and thus small entrance-channel mass asymmetry), all the three observables mentioned are consistent, in that, they all carry signature of the contribution from non-compound nucleus fission which is accompanied by a suppression in the formation of evaporation residues. This suggests very short time-scale of fusion–fission process without complete equilibration in various degrees of freedom. It is the reaction systems involving lighter projectiles for which results obtained using different observables are not mutually consistent [12,13,17,18]. Therefore, it is important to study the reaction systems involving lighter projectiles while investigating the contribution from non-compound nucleus fission/fusion hindrance. Also, it is important to highlight the differences in the (light mass) pre-actinide and (heavy mass) actinide regions in the context of these processes. As mentioned earlier, the onset of non-compound nucleus fission processes in terms of entrance-channel mass asymmetry would be lower in the actinide region compared to that in the pre-actinide region due to the compact saddle point.

In this article, results of our studies on fission fragment angular distribution in ^{16}O+^{188}Os, ^{28}Si+^{176}Yb reactions [19] and fission product mass and angular distributions in ^{20}Ne+^{232}Th reaction [20,21] are discussed in the context of earlier studies involving similar compound nuclei. The first reaction system was chosen, as it lies close to the proposed onset ($Z_PZ_T\sim1000$, Z_P and Z_T are the atomic numbers of the projectile and the target, respectively) of the non-compound nucleus fission based on the measurement of fission fragment mass distribution [7]. The second system (^{20}Ne+^{232}Th) was chosen,

in view of the different observations from the measurement of fission fragment angular distribution [13] and evaporation residue cross-section [18] in the ^{16}O+^{238}U reaction. It should be mentioned here that, the CN masses in [19] and [20,21] are not exactly the same compared to those of the studies in [7] or [13,18]. It is assumed that a small difference of two neutrons would not result in any major effect.

2. Fission fragment angular distribution in ^{16}O+^{188}Os and ^{28}Si+^{176}Yb reactions (pre-actinide region)

In the pre-actinide region, comparable cross-sections for fission and evaporation make it easier to measure different observables, namely, fission fragment mass, angular distributions and evaporation residue cross-section. Rafiei *et al* [7] measured fission fragment mass distribution in different reactions populating the same compound nucleus ^{202}Po. Based on these studies, the onset of the contribution from non-compound nucleus fission was proposed to be around $Z_P Z_T \sim 1000$. In view of this, fission fragment angular distribution was measured in ^{28}Si+^{176}Yb reaction ($Z_P Z_T = 980$) to investigate the contribution from non-compound nucleus fission. In addition, measurements were also carried out for ^{16}O+^{188}Os reaction which is not expected to have any contribution from the non-compound nucleus fission. Data from this reaction were used to fix the input parameters of the theoretical calculations. Measurement of fission fragment angular distribution was carried out using Si detector-based telescopes in the beam energy range of 84–99 MeV ($E_{\mathrm{c.m.}}/V_{\mathrm{b}}$ in the range of 1.05–1.24, $E_{\mathrm{c.m.}}$ and V_{b} are the energies in centre-of-mass frame of reference and entrance channel Coulomb barrier respectively) for ^{16}O+^{188}Os reaction and 138–155 MeV ($E_{\mathrm{c.m.}}/V_{\mathrm{b}}$ in the range of 1.05–1.18) for ^{28}Si+^{176}Yb reaction, respectively. Experiments were carried out using ^{16}O and ^{28}Si beams from BARC–TIFR Pelletron–LINAC Facility at TIFR, Mumbai. Details can be found in [19]. Laboratory angular distributions of fission fragments were transformed into centre-of-mass frame of reference using standard kinematic equations with kinetic energies calculated using the prescription of Rossner *et al* [22]. Centre-of-mass angular distributions of fission fragments were fitted using SSPM equation [4,5]

$$W(\theta) \propto C \sum_{\ell=0}^{\infty} \frac{(2\ell+1)^2 T_\ell \exp\left[-\frac{(\ell+1/2)^2 \sin^2\theta}{4K_0^2}\right] J_0[i(\ell+1/2)^2 \sin^2\theta/4K_0^2]}{(2K_0^2)^{1/2}\mathrm{erf}[(\ell+1/2)/(2K_0^2)^{1/2}]}, \tag{1}$$

where T_ℓ is the transmission coefficient for fission for the ℓth partial wave and K_0^2 is the variance of K distribution, K being the projection of angular momentum vector on the nuclear symmetry axis. J_0 is the zeroeth-order Bessel function. The constant C is a normalization factor. Experimental angular distributions were fitted using eq. (1) with C and K_0^2 as free parameters and from the fitted curves experimental anisotropies were deduced. The compound nucleus ℓ-distribution as calculated using the code CCFUS [23] was used as input in CASCADE [24] calculations to obtain the ℓ-distribution of the fissioning nucleus. The input parameters of CASCADE code were fixed by using the fission cross-section data for ^{16}O+^{188}Os reaction, for which contribution from non-CN fission is expected to be absent. For comparison, angular anisotropies for CN fission were calculated using the theoretical value of K_0^2 based on the statistical saddle-point model. Details

of the calculations can be found in [19]. A comparison of the calculated and experimental anisotropies for ^{16}O+^{188}Os and ^{28}Si+^{176}Yb reactions is shown in figure 1 [19]. It can be seen from the figure that the experimental values are close to the values calculated using SSPM. For the ^{28}Si+^{176}Yb reaction, entrance-channel mass asymmetry (α) is lower compared to the Businaro–Gallone (BG) value (α_{BG}) [25]. For this reaction, pre-equilibrium fission contribution was calculated to be in the range of 7.3–22.4% corresponding to the beam energy range of 138–155 MeV. As seen from figure 1, anisotropy values calculated after including the contribution from pre-equilibrium fission do not deviate significantly from the SSPM values as the expected contribution from pre-equilibrium fission is small. The present observations are consistent with the results obtained in ^{19}F+^{197}Au reaction [17]. Also, it should be mentioned here that experimental anisotropy approaches closer to the value for pre-equilibrium fission with increasing beam energy. Therefore, sensitivity of the angular distribution to the contribution from non-compound nucleus fission will decrease with increasing beam energy. In order to get a comprehensive picture, it is desired to obtain the data on evaporation residue cross-section and spin distribution. Efforts are on in this direction.

3. Fission product mass and angular distributions in ^{20}Ne+^{232}Th reaction

As the fissioning system becomes heavier, the saddle point becomes compact and lower in energy. Due to this, significant contribution from the non-compound nucleus fission may be expected even with the light heavy ions such as ^{16}O. Anomalous fission fragment

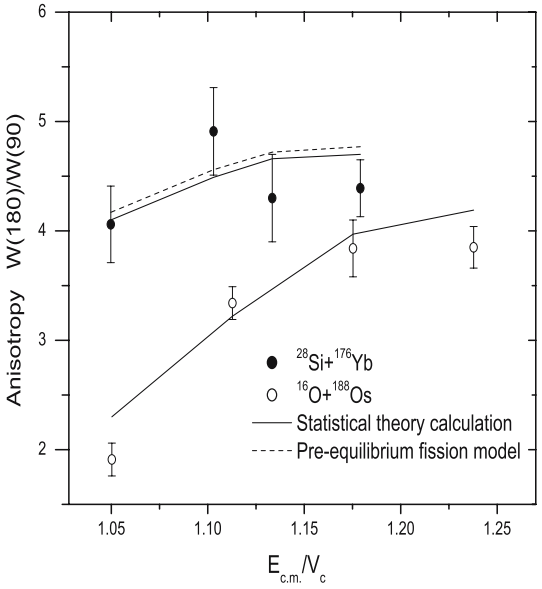

Figure 1. Comparison of the experimental and calculated anisotropies for ^{16}O+^{188}Os and ^{28}Si+^{176}Yb reactions [19]. Solid lines represent calculations based on the statistical saddle-point model (SSPM) [4,5]. Dashed line represents the calculation after including the contribution from pre-equilibrium fission [19].

angular distribution was reported in $^{16}O+^{238}U$ reaction at near and sub-barrier energies [13]. This observation was attributed to the contribution from orientation-dependent quasifission, in which, fissioning system escapes into the exit channel without being captured inside the saddle point [13]. However, no suppression in the evaporation residue cross-section was observed in the measurements by Nishio *et al* [18]. It was proposed in [18] that the anomalous angular distribution may be due to the contribution from pre-equilibrium fission. Thus, angular anisotropy averaged over all the fission products, though, can give information about the contribution from non-compound nucleus fission, it cannot be used to distinguish pre-equilibrium fission and quasifission. As mentioned earlier, basic difference in the mechanism of the two processes lies in the fact that the fissioning system encounters a fission barrier in the pre-equilibrium fission and not in quasifission. This difference in the mechanism may be reflected in the dependence of the angular anisotropy on the asymmetry of mass division and, in turn, on fission product mass. Vorkapic and Ivanisevic [26] explained the mass dependence of angular anisotropy observed in $^{16}O+^{232}Th$ reaction [27] to the variation in fission time-scale with variation in asymmetry of mass division. The largest anisotropies were observed for symmetric fission products, which were attributed to the lower fission barrier and thus least time for K-equilibration. In quasifission, the fissioning system does not encounter a fission barrier and, therefore, such a dependence is not expected. On the other hand, as quasifission leads to a broadening in the fission fragment/product mass distribution or even results in an asymmetric component in the mass distribution [6–12], anomaly in the angular distribution would be expected to be pronounced in the asymmetric mass region. Thus, mass dependence of anisotropy offers a possibility to distinguish between pre-equilibrium fission and quasifission. However, when fissile targets are used there would be contribution from transfer-induced fission involving partial linear momentum transfer, in addition to

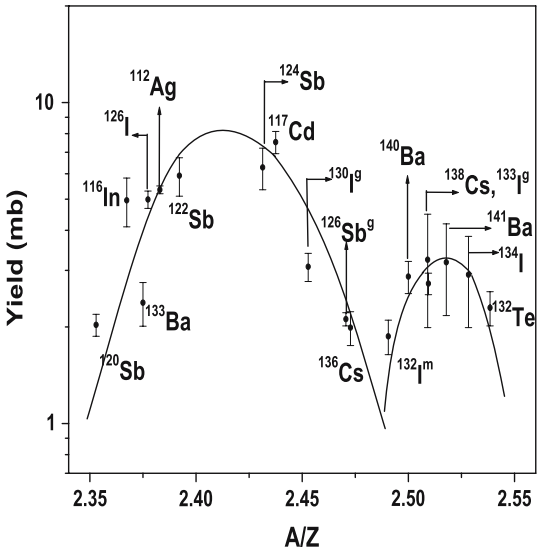

Figure 2. Plot of independent or nearly independent yields of fission products formed in $^{20}Ne+^{232}Th$ reaction at $E_{lab} = 142.5$ MeV as a function of their A/Z. Solid lines are guides to the eye [20].

the non-compound fission processes mentioned earlier. Identification of the fission products with large contribution from transfer-induced fission is necessary to understand the experimental data better. Therefore, mass distribution measurements were also carried out along with the angular distribution measurements. Mass and angular distributions were measured by off-line radiochemical method [20,21].

For mass distribution studies, fission products recoiling out of the target were collected in the aluminium catcher foil. After irradiation both the target and the catcher foils were assayed for the γ-ray activity of the fission products, which were used to obtain their yields. Details can be found in [20]. A plot of independent or nearly independent yield of fission products formed in ^{20}Ne+^{232}Th reaction at $E_{\rm lab} = 142.5$ MeV is shown in figure 2 [20]. As seen from this figure, fission products with $A/Z \gtrsim 2.47$ are expected to be predominantly formed in transfer-induced fission and, therefore, should not be considered while investigating the non-compound nucleus fission. For angular distribution studies, fission fragments were collected in the aluminium catcher foils arranged in a cylindrical geometry in the forward hemisphere. After irradiation, aluminum foils were cut into stripes corresponding to different angles. From the γ-ray activity of the fission products in different catcher foils, their laboratory angular distributions were obtained (details can be found in [21]) which were converted into centre-of-mass frame of

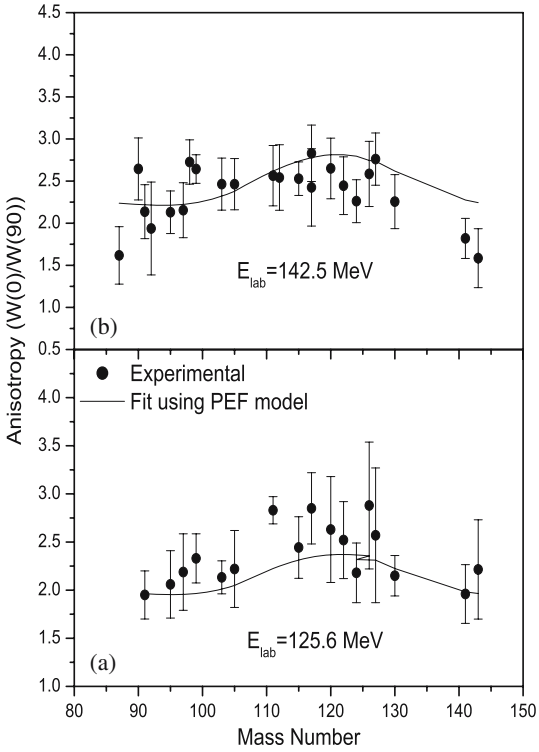

Figure 3. Plot of angular anisotropies of fission products in ^{20}Ne+^{232}Th reaction at (**a**) $E_{\rm lab} = 125.6$ MeV and (**b**) 142.5 MeV [21]. Filled circles represent the experimental data and solid lines represent the theoretical calculations.

reference using standard kinematic equations as was done in the case of on-line measurements. Angular anisotropies of fission products ($A/Z < 2.47$) in ^{20}Ne+^{232}Th reaction obtained by fitting their centre-of-mass angular distributions are shown in figure 3 [21]. Figures 3a and 3b correspond to $E_{\rm lab} = 125.6$ and 142.5 MeV, respectively. Filled circles are the experimental data points. At both the beam energies, average anisotropies were higher compared to those calculated using SSPM indicating the contribution from non-compound nucleus fission [21]. It can be seen from the figure that the angular anisotropies are largest in the symmetric mass region and decrease with the increasing asymmetry of mass division. This observation is consistent with that in the ^{16}O+^{232}Th reaction [27]. This suggests that the observed anomaly in the fission products angular distribution can be attributed to the contribution from pre-equilibrium fission. Theoretical calculations with the incorporation of pre-equilibrium fission were carried out using the model proposed in [28,29]. The details can be found in [21]. The calculations are shown as solid lines in figure 3. It can be seen from the figure that the calculations reasonably reproduce the experimental trend of anisotropies. It would be important to extend these studies to near and sub-barrier energies to investigate the contribution from pre-equilibrium and quasi-fission. Such studies in ^{16}O+^{238}U reaction would help in a better understanding of the results of fission fragment angular distribution [13] and evaporation residue cross-section [18] measurements.

4. Conclusions

Detailed studies on the evaporation residue cross-section and fission fragment/product mass and angular distributions are required to understand the contribution from non-compound nucleus fission in reactions involving lighter projectiles. Such comprehensive measurements are comparatively easier in the pre-actinide region due to comparable cross-sections for fission and evaporation. The measurement of fission fragment angular distribution in ^{28}Si+^{176}Yb reaction showed that the contribution from non-compound nucleus fission is not very large [19]. This is consistent with the observation based on the mass distribution studies in similar compound nucleus populated through different reactions [7]. Measurement of evaporation residue cross-section will give more information on this aspect, particularly about the fusion hindrance in this reaction.

Recent measurements on the mass-resolved angular distribution of fission products in ^{20}Ne+^{232}Th reaction [21] has shown that the mass dependence of the anisotropy offers a possibility to distinguish between pre-equilibrium and quasifission. Mass dependence of the angular anisotropy of fission products in ^{20}Ne+^{232}Th reaction was attributed to the contribution from pre-equilibrium fission. Experimental trend of angular anisotropies could be reasonably explained after incorporating the contribution from pre-equilibrium fission. It would be important, as well as challenging, to extend these studies at near and sub-barrier energies to distinguish the contribution from pre-equilibrium and quasifission.

Acknowledgements

The authors would like to thank all the authors including the coworkers whose works are cited in this article.

References

[1] V S Ramamurthy *et al*, *Phys. Rev. C* **32**, 2182 (1985)
[2] V S Ramamurthy *et al*, *Phys. Rev. Lett.* **65**, 25 (1990)
[3] W J Swiatecki, *Phys. Scr.* **24**, 113 (1981)
[4] R Vandenbosch and J R Huizenga, *Nuclear fission* (Academic Press, London, 1973)
[5] I Halpern and V M Strutinsky, in *Proceedings of the Second United Nations International Conference on Peaceful Uses of Atomic Energy*, Geneva, 1958, edited by J H Martens *et al* (United Nations, Switzerland, 1958) Vol. 15 p. 408
[6] J Toke *et al*, *Nucl. Phys. A* **440**, 327 (1985)
[7] R Rafiei *et al*, *Phys. Rev. C* **77**, 024606 (2008)
[8] K Nishio, H Ikezoe, S Mitsuoka, I Nishinaka, Y Nagame, T Watanabe, T Ohtsuki, K Hirose and S Hofmann, *Phys. Rev. C* **77**, 064607 (2008)
[9] A Yu Chizhov *et al*, *Phys. Rev. C* **67**, 011603(R) (2003)
[10] E Prasad *et al*, *Phys. Rev. C* **81**, 054608 (2010)
[11] T K Ghosh *et al*, *Phys. Rev. C* **69**, 031603 (2004)
[12] A C Berriman *et al*, *Nature* **413**, 144 (2001)
[13] D J Hinde, M Dasgupta, J R Leigh, J P Lestone, J C Mein, C R Morton, J O Newton and H Timmers, *Phys. Rev. Lett.* **74**, 1295 (1995)
[14] D J Hinde, M Dasgupta, J R Leigh, J C Mein, C R Morton, J O Newton and H Timmers, *Phys. Rev. C* **53**, 1290 (1996)
[15] Swaminathan Kailas, *Phys. Rep.* **284**, 381 (1997)
[16] B B Back, R R Betts, J E Gindler, B D Wilkins, S Saini, M B Tsang, C K Gelbke, W G Lynch, M A McMahan and P A Baisden, *Phys. Rev. C* **32**, 195 (1985)
[17] R Tripathi, K Sudarshan, S Sodaye, A V R Reddy, K Mahata and A Goswami, *Phys. Rev. C* **71**, 044616 (2005)
[18] K Nishio, H Ikezoe, Y Nagame, M Asai, K Tsukada, S Mitsuoka, K Tsuruta, K Satou, C J Lin and T Ohsawa, *Phys. Rev. Lett.* **93**, 162701 (2004)
[19] R Tripathi, K Sudarshan, S K Sharma, K Ramachandran, A V R Reddy, P K Pujari and A Goswami, *Phys. Rev. C* **79**, 064607 (2009)
[20] S Sodaye, R Tripathi, K Sudarshan and R Guin, *Phys. Rev. C* **87**, 044610 (2013)
[21] R Tripathi, S Sodaye, K Sudarshan and R Guin, *Phys. Rev. C* **88**, 024603 (2013)
[22] H H Rossner, J R Huizenga and W U Schröder, *Phys. Rev. Lett.* **53**, 38 (1984)
[23] C H Dasso and S Landowne, *Comput. Phys. Commun.* **46**, 187 (1987)
[24] F Puhlhofer, *Nucl. Phys. A* **280**, 267 (1977)
[25] K U L Businaro and S Gallone, *Nuovo Cimento* **5**, 315 (1957)
K T R Davies and A J Sierk, *Phys. Rev. C* **31**, 915 (1985)
[26] D Vorkapic and B Ivanisevic, *Phys. Rev. C* **55**, 1997 (1997)
[27] Bency John *et al*, *Phys. Rev. C* **51**, 165 (1995)
[28] B K Nayak, R G Thomas, R K Choudhury, A Saxena, P K Sahu, S S Kapoor, Raghav Verma and D Umarkanth, *Phys. Rev. C* **62**, 031601 (R) (2000)
[29] R G Thomas, R K Choudhury, A K Mohanty, A Saxena and S S Kapoor, *Phys. Rev. C* **67**, 041601(R) (2003)